Angewandte Chemie
Eine Zeitschrift der Gesellschaft Deutscher Chemiker

Supporting Information

69451 Weinheim, Germany

Ryadnov M. G.
A Self-Assembling Peptide Polynanoreactor of De Novo Design

Notes

SD-1

CD showed a good formation of an α-helix in solution for SD-1 (65%, at 100 μM)[s1] (Fig. S1a). Furthermore, the thermal denaturation of SD-1 followed by CD gave sigmoidal unfolding curves, with their first derivatives being dominated by a single peak with transition midpoints of 60°C (Fig. S1b). The system also exhibited a complete reversibility of unfolding as judged by comparing pre- and post-denaturation CD spectra at 20°C (Fig. S2).

Control sequences

In contrast to SD-1, CD spectra for a control sequence (QEIAALEQEIAALEYEIAALE-am, SD-1A), in which arginine residues were replaced by alanines to eliminate electrostatic networks consolidated by arginines, were indicative of a random coil (Fig. S2). Consistent with this, no assemblies were detected for SD-1A by TEM. Another control sequence (QEIAKLEQEIAKLEYEIAKLE-am, SD-1K) with arginines replaced by lysines was designed. Unlike arginines ε-amino groups of lysines can form only one salt bridge. This interaction is most favoured to be intramolecular as only in this case some helicity can be stabilized through the interactions of *i* to *i+4* or *i* to *i+3* spacings. However, the formation of a coiled coil is disfavoured due to electrostatic repulsions between glutamate residues. Consistent with this, CD showed an unappreciable helical signal, ~10 % (Fig S2a). No assemblies were observed by TEM for either SD-1K or SD-1K in combination with SD-2. This altogether strongly indicates that only the formation of double salt bridges by arginine residues leads to the network of electrostatic interactions as designed.

SD-1 assemblies

Typically for paracrystals,[s2, 3] the SD-1 assemblies proved to be, at least partly, thermotropic: post-melt SD-1 did not immediately re-assemble into supradendrimers. Several hours of incubation at benign conditions were needed for morphologically similar assemblies to become detectable by TEM (Fig. S3b). Furthermore, slight (1-2 units) pH shifts facilitated morphological changes of the phase; hexagons tended to burst into needle-alike fibrils at pH 5-6, whereas overly acidic and alkaline pH completely transferred it into a liquid phase (Fig. S3c&d).

SD-1,2

The assembly of SD-1,2 supradendrimers could be diverted down to smaller associations by slight pH increases, (Fig. S5). As proved by CD, SD-1,2 remained helical and cooperatively folded at pH 10. Gratifyingly, the SD-1,2 assemblies were regenerated by re-buffering to neutral pH.

Silver nanoparticles

Additional high-mag electron micrographs of silver nanoparticles casted in SD-1,2 are presented in Fig S7. No particles were observed under the same conditions in the absence of SD-1,2. Likewise, no formation of colloidal

silver occurred for SD-1 preparations. The latter can be attributed to that SD-1 tends to exhibit thermo- and lyotropic properties as SD-1 assemblies are readily destabilized by increases in temperature or buffer volume. Intriguingly, some smaller clusters of larger colloids of irregular sizes (10-40 nm) were detected for the cysteine-containing SD-1C and similarly for SD-1CA (Fig. S6). This suggests that cysteine residues in the non-assembling peptides should facilitate the reduction of ionic to colloidal silver. This, however, was non-specific and did not prove to be highly reproducible. Nonetheless, this is interesting and may require an independent investigation, which might positively add to a series of studies on peptide-mediated patterning of metallic nanoparticles led by Stone's[s4], Naik's[s5] and Belcher's[s6] groups.

Peptide synthesis

Peptides were synthesized manually using standard Fmoc/*t*Bu/Mtt solid-phase protocols on a Rink amide MHBA resin with HBTU/DIPEA as coupling reagents. SD-2 sequences were assembled on an Ac-Lys-Lys-Lys-Rink amide MBHA via ε-aminohexanoic acids as spacers to give a starburst construct analogously to published ones[s7]. Peptides were purified by RP-HPLC and confirmed by mass-spectrometry (ESI and MALDI-TOF). MS $[M+H]^+$: SD-1 – m/z 2572 (calc), 2572 (found); SD-1C – m/z 2547 (calc), 2548 (found); SD-1A – m/z 2316 (calc), 2317 (found); SD-1AC – m/z 2291 (calc), 2292 (found); SD-1K – 2488 m/z (calc), 2489 (found); SD-2 – m/z 7800 (calc), 7802 (found).

Figures

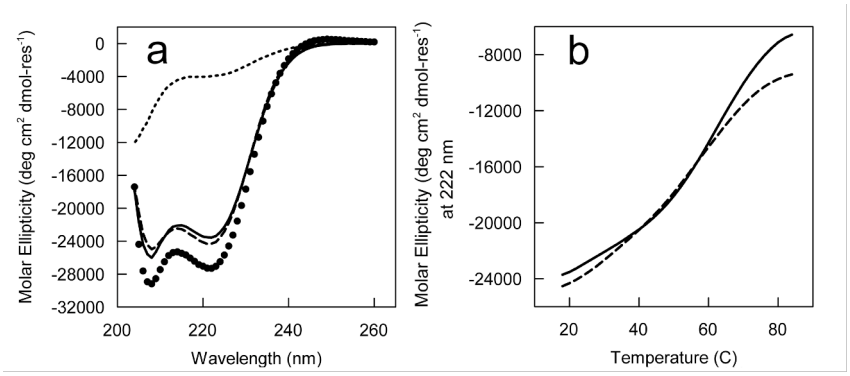

Figure S1. Assembly of supradendrimers assessed by circular dichroism spectroscopy. **a**, spectra recorded at room temperature, pH 7.4 for 100 μm SD-2 (dotted line), SD-1 (bold line), SD-1,2 at 1:0.1 ratio (dashed line) and SD-1,2 at 1:1 ratio (black circles). **b**, thermal unfolding of SD-1 (bold line) and SD-1,2 at 1:0.1 ratio (dashed line). The first derivatives of the curves gave Tm values of 60 and 64 °C, respectively. $-100([\theta]_{222} + 3000)/33000$ was used to calculate the percent α-helix[s1]

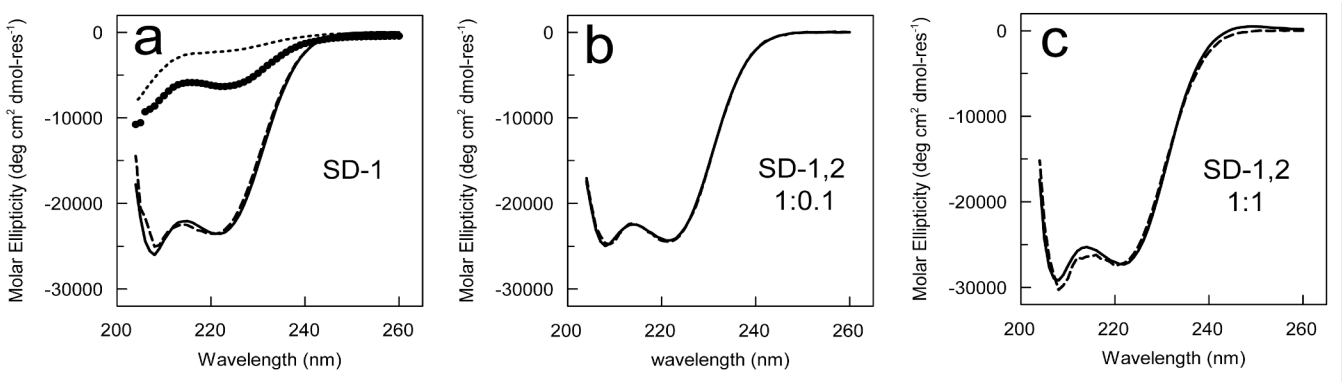

Figure S2. Pre- (solid lines) and post- (broken lines) denaturation CD spectra of SD-1 (**a**) and SD-1,2 (**b**, **c**) supradendrimers. (**a**) SD-1A (dotted line) and SD-1K (black circles) at benign conditions. All spectra are for 100 μM peptide (10 μM for SD-2 in **b**), pH 7.4, 20 °C.

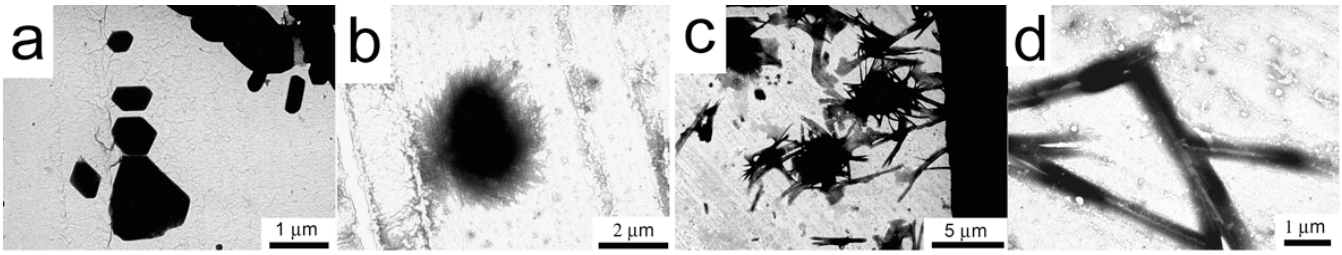

Figure S3. Electron micrographs of SD-1 supradendrimers. **a**, at benign conditions; **b**, annealed at benign conditions; **c**, at pH 5.3; **d**, needle-alike fibrils at pH 5.3.

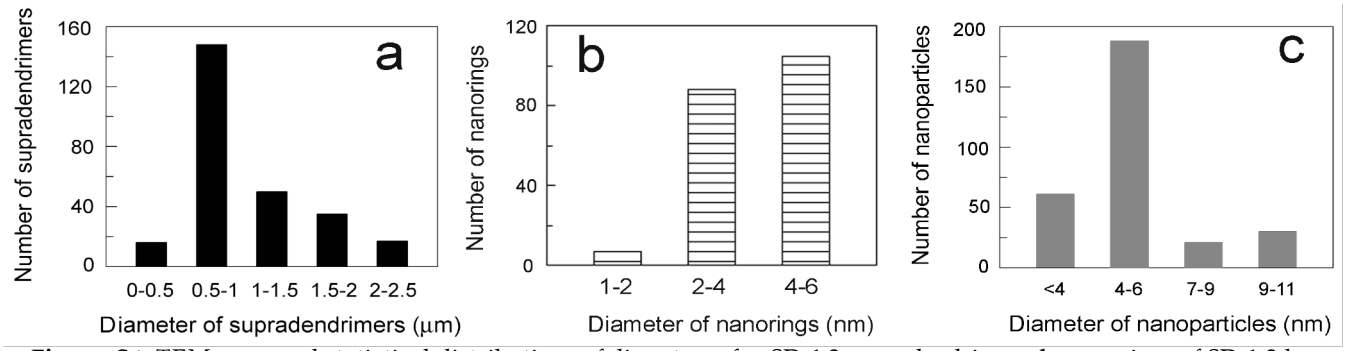

Figure S4. TEM-measured statistical distributions of diameters of **a**, SD-1,2 supradendrimers; **b**, nanorings of SD-1,2 branching cells; **c**, silver nanoparticles. The sizes of the bins are ± 150, 0.7 and 1 nm, respectively. The average diameters were calculated from the breakdowns of these data as 1.4 ± 0.4 microns, 4.6 ± 0.7 nm, 5.2 ± 0.5 nm, respectively.

Figure S5. Maturation (**a**-**c**) and disassembly (**c**-**e**) of SD-1,2 supradendrimers. **a**, smaller SD-1,2 assemblies (hypothetical nuclei)

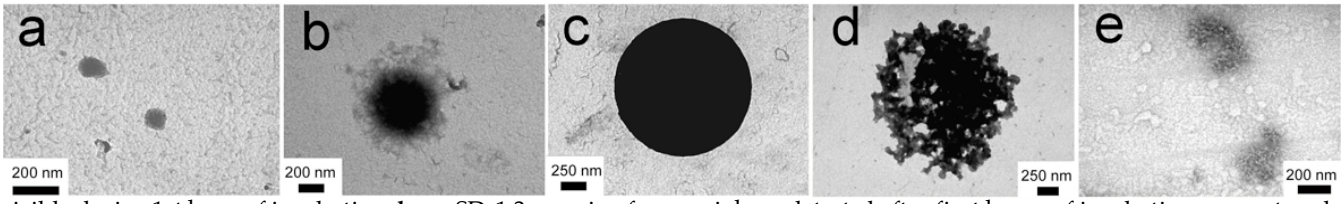

visible during 1st hour of incubation; **b**, an SD-1,2 growing from periphery detected after first hours of incubation; **c**, a matured SD-1,2; **d**, partly disintegrated SD-1,2 at pH 8.6; **e**, a disassembled SD-1,2 at pH 10.

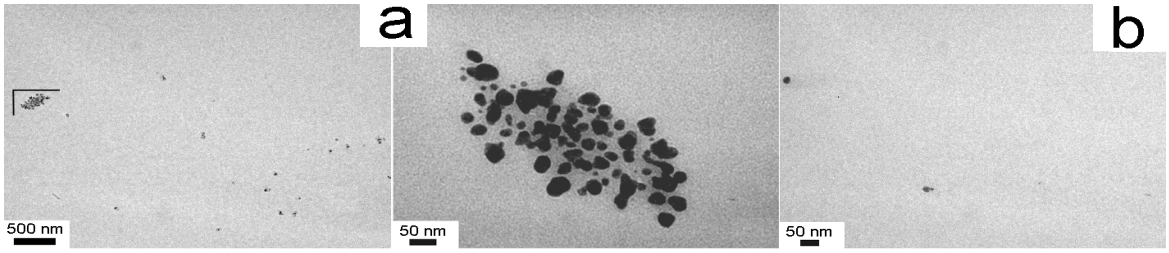

Figure S6. Clusters of colloidal silver formed in the presence of SD-1C (**a**) and SD-1CA (**b**).

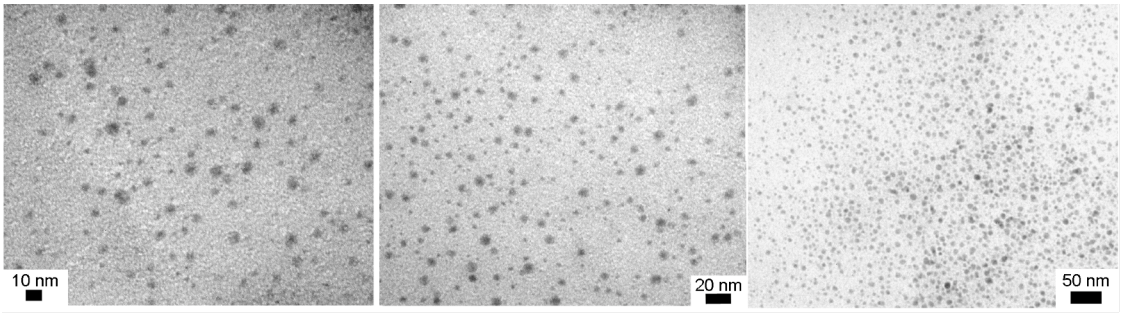

Figure S7. Enlarged electron micrographs of silver nanoparticles casted within SD-1,2 polynanoreactors.

References

[s1] J. D. Morrisett, R. L. Jackson, J. Gotto, A. M., *Biochimica et Biophysica Acta (BBA) - Reviews on Biomembranes* **1977**, *472*, 93.
[s2] A. M. Hindeleh, Hosemann, R., *J. Phys. C: Solid State Phys.* **1988**, *21*, 4155.
[s3] H. Herrmann, U. Aebi, *Ann. Rev. Biochem.* **2004**, *73*, 749.
[s4] R. R. Naik, Stringer, S. J., Agarwal, G., Jones, S. E. & Stone, M. O., *Nature Mater.* **2002**, *1*, 169.
[s5] R. M. Kramer, C. Li, D. C. Carter, M. O. Stone, R. R. Naik, *J. Am. Chem. Soc.* **2004**, *126*, 13282.
[s6] S. R. Whaley, D. S. English, E. L. Hu, P. F. Barbara, A. M. Belcher, *Nature* **2000**, *405*, 665.
[s7] M. G. Ryadnov, D. N. Woolfson, *J. Am. Chem. Soc.* **2005**, *127*, 12407.